Strong exciton-photon coupling in a monolithic ZnO/(Zn,Mg)O multiple quantum well microcavity

S. Halm, S. Kalusniak, S. Sadofev, H.-J. Wünsche, and F. Henneberger

Citation: Appl. Phys. Lett. **99**, 181121 (2011); doi: 10.1063/1.3657527
View online: http://dx.doi.org/10.1063/1.3657527
View Table of Contents: http://apl.aip.org/resource/1/APPLAB/v99/i18
Published by the American Institute of Physics.

Strong exciton-photon coupling in a monolithic ZnO/(Zn,Mg)O multiple quantum well microcavity

S. Halm,[a] S. Kalusniak, S. Sadofev, H.-J. Wünsche, and F. Henneberger
Institut für Physik, Humboldt Universität zu Berlin, D-12489 Berlin, Germany

(Received 27 June 2011; accepted 12 October 2011; published online 3 November 2011)

We report on strong exciton-photon coupling in an epitaxially grown (Zn,Mg)O-based λ-microcavity (MC) containing four 3.5 nm wide ZnO quantum wells (QWs) as active layers. At 5 K, the observed Rabi splitting in absorption is 26 meV, while the inhomogeneous linewidth of A and B excitons in similar QWs without a MC is about 10 meV. The strong coupling regime (SCR) is lost between 150 K and 200 K due to additional homogeneous broadening. From transfer matrix calculations, we deduce that increasing the number of QWs per cavity length can extend the SCR up to room temperature.
 [doi:10.1063/1.3657527]

During the past decades, strong exciton-photon coupling in semiconductor microcavities (MCs) has been subject of extensive research.[1] The quest has led to the discovery of many fascinating effects in CdTe and GaAs-based multiple quantum well (MQW) MCs, such as optical parametric oscillation,[2–4] Bose-Einstein condensation,[5,6] and polariton suprafluidity.[7] However, due to the materials used, these effects were limited to cryogenic temperatures, which is why wide band gap semiconductors like GaN and ZnO with large oscillator strength and stable excitons at room temperature (RT) came into focus. By now, e.g., polariton lasing at RT has been demonstrated in a GaN MC (Ref. 8) and plausible evidence for Bose-Einstein condensation could be given.[9] While in the GaAs, CdTe, and GaN systems, MQW active layers are frequently employed, strong exciton-photon coupling in ZnO has so far only been reported for bulk active layers in hybrid MCs.[10–12] MQW structures can offer various advantages over bulk material, such as an enhanced binding energy and oscillator strength, tunability of the exciton resonance, and the possibility to position the quantum wells (QWs) at the electric field antinodes of the MC. Their growth is more challenging though, since QWs usually suffer from inhomogeneous broadening. In previous work, it was shown that epitaxial growth of high optical quality ZnO/(Zn,Mg)O QWs is feasible via molecular beam epitaxy.[13,14] Recently, we fabricated (Zn,Mg)O-based distributed Bragg reflectors (DBRs) and achieved vertical cavity surface emitting laser (VCSEL) action in an all monolithic ZnO-based MC using QWs as active layers.[15]

In this letter, we demonstrate that strong exciton-photon coupling is obtained in a monolithic ZnO MQW MC, similar to the VCSEL structure in Ref. 15, up to a temperature of $T \approx 150$ K. We use angle resolved reflectivity and transmission spectroscopy to determine the MC dispersion in absorption between 5 K and 300 K. For reference, we additionally record the absorption spectra of a similar MQW structure without a cavity and use the results to simulate the MC properties with the transfer matrix method (TMM).[16] Finally, we study the prospect of reaching the strong coupling regime (SCR) at RT.

The samples are grown by molecular beam epitaxy on *a*-plane $(11\bar{2}0)$ sapphire substrates at a low growth temperature of $T_g \approx 340\,^{\circ}$C. The MC sample A contains a λ-cavity of $Zn_{0.92}Mg_{0.08}O$ and includes four 3.5 nm wide ZnO QWs positioned near the antinodes of the electric field. The cavity is sandwiched between a lower and an upper DBR consisting of 20 and 18 $Zn_{1-x}Mg_xO$ bilayers ($x_1 = 0.08$, $x_2 = 0.35$), respectively. A schematic sample layout is shown in Fig. 1(a). The reference MQW (sample B) consists of five 3.7 nm wide ZnO QWs with 11 nm wide $Zn_{0.92}Mg_{0.08}O$ barriers grown on a 670 nm $Zn_{0.92}Mg_{0.08}O$ buffer and capped by 37 nm of the barrier material. Details on growth can be found in Ref. 15. Good structural quality of the monolithic (Zn,Mg)O MC is confirmed by atomic force microscopy (AFM) and scanning electron microscopy (SEM). As can be seen in Fig. 1(b), the surface of the 3.56 μm thick MC structure is flat within a few nanometers, which strongly suppresses scattering of light. The root mean square roughness over a scan area of $(15\,\mu\text{m})^2$ amounts to 1.2 nm. In cross section SEM (Fig. 1(c)), the DBR layers exhibit regular periodicity and abrupt interfaces.

Sample A is mounted in a transmission helium flow cryostat which allows for temperature control between 4 K and 300 K. Angle resolved reflectivity R and transmission $\mathcal{T}$ are recorded by a home-built goniometer setup with an angular resolution of about $\pm 1^{\circ}$. The spectra collected at 5 K with transverse-electric (TE) polarized light are depicted in Figs. 2(a) and 2(b). After confirming that $R + \mathcal{T} = 1.00 \pm 0.02$ holds in the spectral region where the sample is transparent, we determine absorption by $A = 1 - R - \mathcal{T}$, see Fig. 2(c). At the given sample position, the detuning δ, defined as the difference between the uncoupled cavity (E_c) and exciton (E_x) resonance energies, amounts to $\delta = E_c - E_x \approx -54$ meV, and the resonance condition is met at an angle of $\theta \approx 32^{\circ}$ ($\sin\theta = 0.53$). An anticrossing in the dispersion relation with the occurrence of both lower and upper polariton branches is observed in R as well as in A. Note that only the latter finding provides unambiguous evidence for the presence of strong exciton-photon coupling in our sample at low temperature.[1] The minimum energy splitting between the polariton branches in A equals $\Omega_r = 26$ meV.

With the help of a TMM model, a detailed account of the MC response can be given. We describe the refractive

[a]Electronic mail: halm@physik.hu-berlin.de.

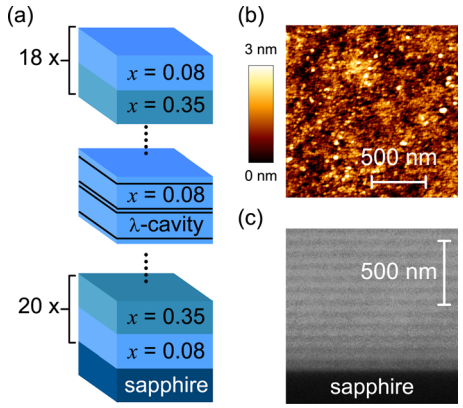

FIG. 1. (Color online) Layout and structural properties of a (Zn,Mg)O MC. (a) Schematic sample layout (not true to scale). (b) AFM image of a $(1.5\,\mu m)^2$ sized region of the MC surface. (c) Cross section SEM image (backscattered electrons) of lower DBR layers.

index dispersion $n(E)$ of the DBR layers by first-order Sellmeier relations (parameters at 5 K obtained by the procedure described in Ref. 15). For the ZnO QWs, the imaginary part $\kappa(E)$ of the complex index of refraction near the exciton resonance is taken from the absorption spectrum $\alpha(E)$ of sample B at 5 K (see Fig. 3(a)). The real part $n(E)$ is obtained by modeling $\alpha(E)$ with a single Voigt profile[17] and a band edge, assuming a (in)homogeneous linewidth of $2\gamma_h = 2$ meV ($2\gamma_i = 17$ meV) and a background refractive index of $n_b = 2.4$. Using reasonable MC structure parameters, very good agreement between experiment (Figs. 2(a)–2(c)) and TMM (Figs. 2(d)–2(f)) is achieved for R, $\mathcal{T}$, and A, respectively. The calculated polariton branches, for example, agree with experiment within 5 meV or less.

While at low temperature for a properly designed sample, lower and upper polariton branches can clearly be resolved, identification of strong coupling at higher T is more challenging: The polariton branches near the exciton resonance are broad, and the upper branch is strongly damped by higher excitonic states. In Fig. 3, we carefully study the continuous evolution of the MC dispersion and its transition from strong to weak coupling between 5 K and 200 K. To begin with, we measure normal incidence absorption of the bare MQW

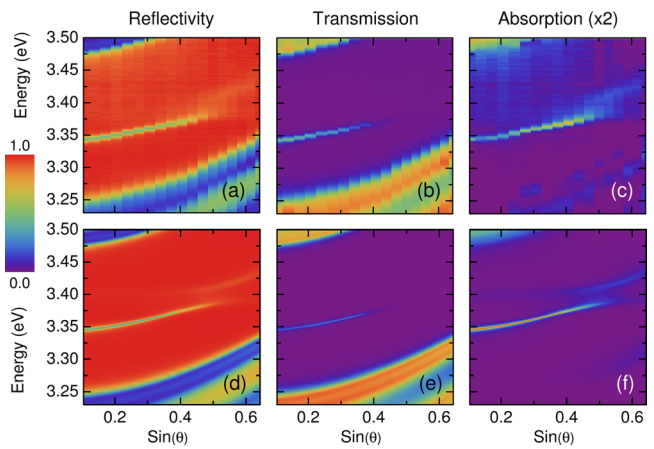

FIG. 2. (Color online) Angle resolved reflectivity, transmission and absorption spectra of the MC in TE polarization at $T = 5$ K. Experimental and simulated results are shown in (a)–(c), and (d)–(f), respectively. Absorption data are multiplied by a factor of 2 for better visibility.

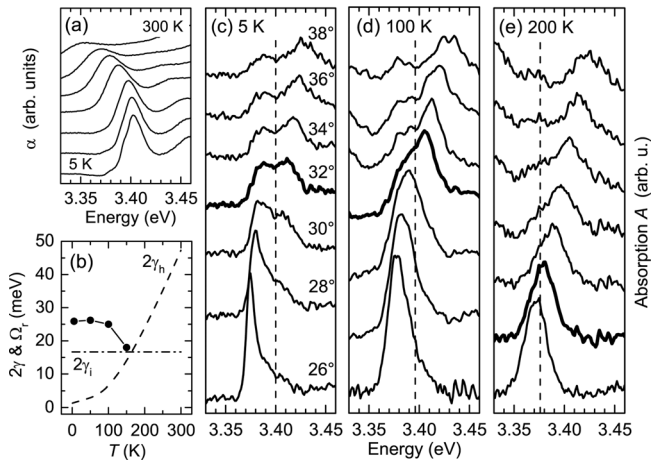

FIG. 3. Transition from strong to weak exciton-photon coupling in the MC. (a) Temperature dependent excitonic absorption of the bare ZnO MQW (sample B) in steps of 50 K. (b) Inhomogeneous ($2\gamma_i$, dashed-dotted line) and homogeneous ($2\gamma_h$, dashed line) Voigt model linewidths to describe the bare MQW absorption, as well as splitting Ω_r between the MC polariton branches at resonance (circles) vs. T. (c-e) Angle resolved MC absorption spectra in the vicinity of the exciton-photon resonance at $T = 5$ K, 100 K, and 200 K, respectively. The dashed lines mark the uncoupled exciton resonance.

(sample B), see Fig. 3(a). The absorption resonance is formed by the spectrally overlapping ground states of A and B excitons, and hence both components participate in the coupling. At 5 K, an indication of the individual contributions can still be observed in form of a peak and a shoulder positioned 8 meV below.[18] The second shoulder appearing at 3.379 eV is attributed to negatively charged trions. A and B excitons exhibit an inhomogeneous broadening due to QW thickness and barrier composition fluctuations with a full width at half maximum (FWHM) of about 10 meV each. At higher T, phonon induced homogeneous broadening becomes dominant. We confirmed that the excitonic ground-state absorption is well-described by a single Voigt profile, when assuming a constant inhomogeneous linewidth $2\gamma_i = 17$ meV and the temperature dependent homogeneous linewidth $2\gamma_h(T)$ from Ref. 19 (see Fig. 3(b), dashed-dotted and dashed lines, respectively).

MC absorption spectra at angles around the exciton-photon resonance are shown in Figs. 3(c)–3(e) for $T = 5$ K, 100 K, and 200 K, respectively. The dashed lines indicate the spectral position of the uncoupled excitonic absorption maximum $E_x(T)$. $E_x(5\,\text{K})$ is set to the center between the upper and lower polariton branches at the resonance angle $\theta_r = 32°$, and for higher T, it is red-shifted by an amount obtained from Fig. 3(a). The absorption spectra closest to resonance are highlighted in bold. To correctly interpret the MC data, the different origin of the excitonic linewidth $2\gamma_x$ at low and high temperatures has to be taken into account. At 5 K, a pronounced splitting Ω_r indicative of the SCR is again visible, but *inhomogeneous* broadening prevails here $\gamma_x \approx \gamma_i$. In this case, the polariton lifetime is known to be only partially affected by γ_i,[20] which, e.g., reduces the effect of wave vector uncertainty.[21] *Homogeneous* broadening dominates the exciton linewidth $\gamma_x \approx \gamma_h$ at $T \geq 200$ K. Ω_r can then be described by[22]

$$\Omega_r = 2\sqrt{V^2 - (\gamma_x^2 + \gamma_c^2)/2}, \quad (1)$$

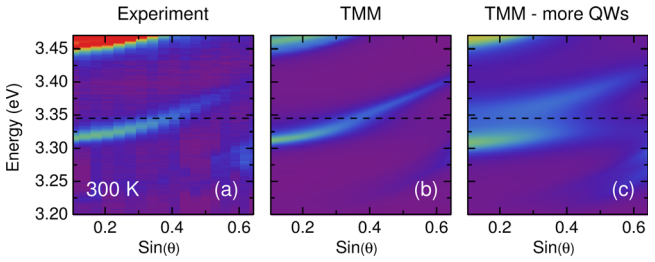

FIG. 4. (Color online) MC absorption at 300 K. (a) Experimental results. (b) TMM calculation. (c) TMM for a MC containing 3 times more QWs. The dashed lines indicate the uncoupled exciton resonance; the color scale is identical to Fig. 2(c).

where V and γ_c are the exciton-photon coupling strength and the homogeneous cavity mode broadening, respectively. The condition for strong exciton-photon coupling[1] $V^2 > (\gamma_x^2 + \gamma_c^2)/2$ is then identical to a finite splitting in absorption Ω_r. Hence, from the observation of vanishing Ω_r at 200 K in Fig. 3(e), we conclude that the SCR is lost at about this temperature. Interestingly, the transition from strong to weak coupling is far from being abrupt: At angles $\theta < \theta_r$, the visibility of the upper branch continuously diminishes with T, while for $\theta > \theta_r$, the lower branch remains visible but shifts onto the bare exciton absorption. The temperature dependence of Ω_r is included by circles in Fig. 3(b).

As shown in Fig. 4(a), no signs of the SCR remain at 300 K, only the unsplit cavity resonance is observed. Using the RT MQW absorption spectrum from Fig. 3(a), experimental results can again be well-reproduced by the TMM.[23] In order to estimate the potential of our monolithic MQW MCs for strong coupling at RT, we increase the QW number in the TMM by a reasonable factor of 3 and thereby the coupling strength by a factor of $\sqrt{3}$.[1] From the reappearance of the two polariton branches in Fig. 4(c), we deduce that our all-monolithic approach is in fact suited to reach the SCR, even though the effective cavity length is larger than in an analogous design involving dielectric DBRs with a higher refractive index contrast. Moreover, the optical quality of our QWs is such that both polariton branches should be observable, allowing for direct experimental access to the splitting of the branches and hence to the coupling strength.

In conclusion, we have shown that monolithic MQW-based (Zn,Mg)O MCs are capable of strong exciton photon coupling. For the present design, the strong-coupling regime is limited to cryogenic temperatures where inhomogeneous broadening of the exciton state is predominant. The temperature-induced homogeneous broadening destroys the strong coupling above 150 K. Increasing the number of QWs or their oscillator strength will allow to overcome this limitation and to realize robust polariton states in these MCs at RT and beyond.

The authors would like to thank P. Schäfer and H. Spranger for SEM and AFM images, respectively.

[1]*Physics of Semiconductor Microcavities: From fundamentals to Nanoscale Devices*, edited by B. Deveaud (Wiley-VCH, Weinheim, 2007).
[2]P. G. Savvidis, J. J. Baumberg, R. M. Stevenson, M. S. Skolnick, D. M. Whittaker, and J. S. Roberts, Phys. Rev. Lett. **84**, 1547 (2000).
[3]M. Saba, C. Ciuti, J. Bloch, V. Thierry-Mieg, R. André, L. S. Dang, S. Kundermann, A. Mura, G. Bongiovanni, J. L. Staehli, and B. Deveaud, Nature (London) **414**, 731 (2001).
[4]C. Diederichs, J. Tignon, G. Dasbach, C. Ciuti, A. Lemaître, J. Bloch, Ph. Roussignol, and C. Delalande, Nature (London) **440**, 904 (2006).
[5]J. Kasprzak, M. Richard, S. Kundermann, A. Baas, P. Jeambrun, J. M. J. Keeling, F. M. Marchetti, M. H. Szymańska, R. André, J. L. Staehli, V. Savona, P. B. Littlewood, B. Deveaud, and Le Si Dang, Nature (London) **443**, 409 (2006).
[6]H. Deng, D. Press, S. Götzinger, G. S. Solomon, R. Hey, K. H. Ploog, and Y. Yamamoto, Phys. Rev. Lett. **97**, 146402 (2006).
[7]A. Amo, J. Lefrère, S. Pigeon, C. Adrados, C. Ciuti, I. Carusotto, R. Houdré, E. Giacobino, and A. Bramati, Nat. Phys. **5**, 805 (2009).
[8]S. Christopoulos, G. Baldassarri Höger von Högersthal, A. J. D. Grundy, P. G. Lagoudakis, A. V. Kavokin, J. J. Baumberg, G. Christmann, R. Butté, E. Feltin, J.-F. Carlin, and N. Grandjean, Phys. Rev. Lett. **98**, 126405 (2007).
[9]J. J. Baumberg, A. V. Kavokin, S. Christopoulos, A. J. D. Grundy, R. Butté, G. Christmann, D. D. Solnyshkov, G. Malpuech, G. Baldassarri Höger von Högersthal, E. Feltin, J.-F. Carlin, and N. Grandjean, Phys. Rev. Lett. **101**, 136409 (2008).
[10]R. Shimada, J. Xie, V. Avrutin, Ü. Özgür, and H. Morkoç, Appl. Phys. Lett. **92**, 011127 (2008).
[11]S. Faure, C. Brimont, T. Guillet, T. Bretagnon, B. Gil, F. Mdard, D. Lagarde, P. Disseix, J. Leymarie, J. Zuñiga-Pérez, M. Leroux, E. Frayssinet, J. C. Moreno, F. Semond, and S. Bouchoule, Appl. Phys. Lett. **95**, 121102 (2009).
[12]C. Sturm, H. Hilmer, R. Schmidt-Grund, and M. Grundmann, New J. Phys. **11**, 073044 (2009).
[13]C. Morhain, X. Tang, M. Teisseire-Doninelli, B. Lo, M. Laügt, J.-M. Chauveau, B. Vinter, O. Tottereau, P. Vennéguès, C. Deparis, and G. Neu, Superlattices Microstruct. **38**, 455 (2005).
[14]S. Sadofev, S. Blumstengel, J. Cui, J. Puls, S. Rogaschewski, P. Schäfer, Yu. G. Sadofyev, and F. Henneberger, Appl. Phys. Lett. **87**, 091903 (2005).
[15]S. Kalusniak, S. Sadofev, S. Halm, and F. Henneberger, Appl. Phys. Lett. **98**, 011101 (2011).
[16]M. Born and E. Wolf, *Principles of Optics*, 6th ed. (Pergamon, Oxford, 1993).
[17]L. C. Andreani, G. Panzarini, A. V. Kavokin, and M. R. Vladimirova, Phys. Rev. B **57**, 4670 (1998).
[18]We attribute the apparent dominance of the B exciton to its superposition with the high energy tail of the asymmetrically shaped A exciton resonance.
[19]R. Hauschild, H. Priller, M. Decker, J. Brückner, H. Kalt, and C. Klingshirn, Phys. Status Solidi C **3**, 976 (2006).
[20]Z. Kurucz, J. H. Wesenberg, and K. M. Mølmer, Phys. Rev. A **83**, 053852 (2011).
[21]V. M. Agranovich, M. Litinskaia, and D. G. Lidzey, Phys. Rev. B **67**, 085311 (2003).
[22]V. Savona, L. C. Andreani, P. Schwendimann, and A. Quattropani, Solid State Commun. **93**, 733 (1995).
[23]The MQW dielectric function at 300 K is determined in the same way as for 5 K. The Voigt model parameters used to obtain $n(E)$ are taken from Fig. 3(b), the background refractive index is set to $n_b = 2.18$.